Journal of Theoretical and Applied Mechanics, Sofia, Vol.51 (2021) pp. 301-316
FLUID MECHANICS

HYDRODYNAMIC STABILITY OF A PERIODIC CHANNEL FLOW OF VISCOELASTIC FLUID

ABDESSAMADE RAFIKI[1*], AHMED HIFDI[2],
YOUSSEF HADDOUT[1], YOUSSEF BELKASSMI[1]

[1]*Research Team ERMAM, Polydisciplinary Faculty of Ouarzazate Box 638, Ibn Zohr University, Morocco*

[2]*Laboratory of Mechanics, University Hassan II-Casablanca, Morocco*

[Received: 17 February 2020. Accepted: 05 April 2021]

ABSTRACT: The local linear stability approaches and the combined effects of a periodic channel modulation and fluid elasticity are investigated on the stability of plane Poiseuille flow of a second-order and second-grade fluids. The fourth order modified Orr-Sommerfeld equation is solved using a spectral method. The critical values of a Reynolds number and a wavenumber are computed for several values of an elasticity number, K and at different section x. According to the channel section, we find that the channel amplitude has a stabilizing or destabilizing effect on the fluids flow. The Y-shaped structure of spectrum of Newtonian fluid flow is remarquabely modified by the elasticity of these fluids. This investigation proves the existence of a dangerous station of the flow corresponding to $x_c = 3\pi/2n$ whith $n = 0.1$.

KEY WORDS: Continuous spectrum, Local stability analysis, Periodic channel, Spectral methode, Viscoelastic fluid.

1 INTRODUCTION

The use of viscoelastic fluids in various technological processes, and the possibility of an appreciable reduction in turbulent friction in polymeric flows, has attracted considerable attention to study the transition from a laminar to a turbulent flow regime. Understanding the combined effect of inertia and viscoelasticity is of great importance, especially in the case of parallel shear flows. Since its discovery by Toms [1] in 1948, the reduction of turbulent drag, induced by a small amount of certain high molecular weight compounds, has been extensively investigated. To illustrate the effect of fluid elasticity on the transition from a laminar to a turbulent flow regime Chun et *al.* [2], Sadeghy et *al.* [3] and Rafiki et *al.* [4, 5] studied the flow stability of two simple models of viscoelastic fluids. In the first so-called "second-order" (SO) model, the appropriateness of parameters used is verified by the experimental

*Corresponding author e-mail: abs.rafiki@gmail.com

data, which is why this model is widely used to model a Non-Newtonian fluid [6–8]. However, Fosdick and Rajagopal [9] show that this model violates certain thermodynamics constrains.

The so-called "second-grade" (SG)rheological models has been proposed by Dunn and Rajagopal [10] as a remedy to comply with thermodynamics, although, it has never been tested experimentally. Recently, there has been an applied mathematical trend towards using the SG fluids model as an equivalent to the Navier-Stokes-alpha (NS-alpha) turbulence model. There are references [11–13] that discuss the relationship between the SG fluids model and the NS-alpha model system, which named the viscous Camassa-Holm equation (VCHE), also known as the Lagrangian averaged Navier-Stokes-model (LANS-alpha). The NS-alpha model equations emerge from the original Navier-Stocks equations by using the specially filtered fluid velocity U_f instead of the unfiltered velocity V_f, when U_f and V_f are related by the Holmholtz operator such as $V_f = (1 - \alpha^2\Delta)U_f$. The physical interpretation of U_f and V_f as Euler and Lagrangian velocity are given in [13]. The VCHE profiles are consistent with data obtained from turbulent channel or pipe flow measurements and simulations [14–16]. Despite its similarity to the rheology of SG fluids, the alpha parameter in the NS-alpha model is a flow regime parameter [11]. Furthermore, Camassa and Holm [17] provided the interpretation of alpha as the typical mean amplitude of the velocity fluctuations. Indeed, the SG fluid model provides a lot of opportunities to have a physically correct interpretations as far as its equations, introduced by Rivlin and Erickson [18], are mathematically identical to the VCHE. For these reasons, the study of the SG fluid model equation is of interest in applied mathematics. In general, for SO fluids, it is found that the fluid elasticity has a destabilizing effect on the flow and that of SG fluid is predicted to have a stabilizing effect.

The linear stability of viscoelastic flows through porous media are encountered in enhanced oil recovery, composites manufacturing and biological transport processes. This has motivated investigation of viscoelastic flows through model geometries, such as periodic channel [19–23]. Experimentally, it is well known that in polymer flows through periodic channel geometries there is an improvement in the pressure drop due to elastic effects [22]. Therefore, these geometries continue to provide rigorous testing of viscoelastic equations and serve as a reference for excellent numerical simulation algorithms. Under such conditions Sureshkumar [24] studied the local linear stability analyses of viscous and viscoelastic flows through a periodically constricted channel. Using the pseudo-spectral method of Chebyshev, it was find that the periodic modulation has a destabilizing effect on the flow.

In the present work, we study the local linear hydrodynamic stability of a periodic channel flow of second-order (SO) and second grade (SG) fluids. Our study mainly focuses on the combined effect of periodic modulation and fluid's elasticity on the

local linear stability of Poiseuille flow. In this context, we investigate the influence of geometric and rheological parameters on Poiseuille flow stability, eigenspectrum as well as near-wall perturbation vorticity. Chebyshev's spectral collocation method is used to solve the eigenvalues problem. This method forms a family of discretization methods for solving ordinary or partial differential equations. They are based on the representation of the solution in a generally polynomial base. The collocation points, which we use, are those of Gauss-Lobatto [25]. One limitation of these methods is that the discretization of partial differential equations leads to the solution of large systems of linear or nonlinear equations involving full matrices. Another drawback of spectral methods is their inability to handle irregularly shaped domains. This is the reason why these methods have had limited use in many engineering problems. Although there have been attempts to use spectral methods in irregular domains [26, 27].

This paper is organized as follows. In Section 2 we describe the geometry of the flow domain, we discuss the governing equations and we determine the basic flow. In Section 3 we present the linear stability analysis in which flow control parameters, generalized eigenvalue problem and computational methods employed in the spatial discretization are determined. Section 4 contains the results and discussion. Conclusions are presented in Section 5.

2 Hydrodynamic Stability of a Periodic Channel Flow of Viscoelastic Fluid

A cartesian coordinate system (x, y) is chosen such that the origin, O, is a midway between the plates with the x-axis in the direction of the flow, the y-axis is perpendicular to the plates and the z-axis in the neutral direction. Considering the Poiseuille flow of a viscoelastic incompressible fluid in a rigid periodic channel where the walls equations are the form:

$$y_w \equiv \pm H[1 + \gamma \sin(nx)]\,, \tag{1}$$

where H is the average half height of the channel, γ is the channel walls amplitude, $n = \frac{2\pi}{L}$ is the dimensionl wavenumber and L is the wavelength in the axial x-direction.

The periodic domain is defined as it is shown in Fig. 1.

The equations governing the fluid motion in dimensional form are given by

$$\rho[\frac{\partial \mathbf{V}}{\partial t} + \mathbf{V} \cdot \nabla \mathbf{V}] = -\nabla p^* + \nabla \cdot \tau\,, \tag{2}$$

$$\nabla \cdot \mathbf{V} = 0\,, \tag{3}$$

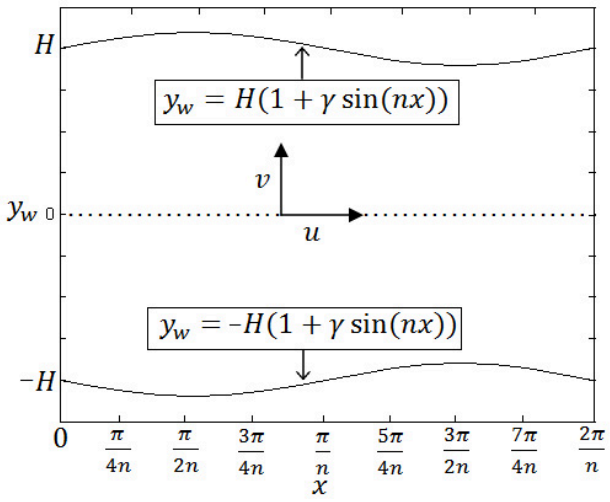

Fig. 1: Geometric domain description in Cartesian coordinates.

where ρ is the fluid density, p^* is the isotropic pressure, $\mathbf{V}(u^*, v^*)$ is the velocity vector and τ is the extra-stress, defined by:

$$\tau = \mu \mathbf{E_1} + \beta_1 \mathbf{E_2} + \beta_2 \mathbf{E_1}^2 , \tag{4}$$

where μ, β_1 and β_2 are measurable material constants of the fluid representing, respectively, the dynamic viscosity, the elasticity and the cross viscosity. The quantities $\mathbf{E_1}$ and $\mathbf{E_2}$ are kinematical tensors defined by

$$\mathbf{E_1} = \nabla \mathbf{V} + (\nabla \mathbf{V})^T ,$$
$$\mathbf{E_2} = \frac{dj}{dt}\mathbf{E_1} = \frac{D}{Dt}(\mathbf{E_1}) + \mathbf{E_1} \cdot \nabla \mathbf{V} + (\nabla \mathbf{V})^T \cdot \mathbf{E_1} ,$$

where $\mathbf{E_1}$ is the deformation rate tensor, $\frac{d_j}{dt}$ is the Jaumann derivative and $\frac{D}{Dt}$ is the material derivative.

It should be noted that under the law of behavior defined by equation (4), two cases are often considered:

i) For SO fluids the $\beta_1 \leq 0$ and $\beta_2 \leq 0$.

ii) For SG fluids $\beta_1 > 0$ and $(\beta_1 + \beta_2) = 0$.

The above equations is associated with the following boundary conditions:

$$u^*(x, y_w) = v^*(x, y_w) = 0 \quad \texttt{and} \quad u^*(x + \frac{2\pi}{n}, y) = u^*(x, y)\,. \tag{5}$$

In the limit where the amplitude of the channel is very inferior to the unity $\gamma \ll 1$, we consider a stationary and unidirectional flow to establish the basic solution of the problem. Taking into account the equations (3), (4) and (5), the resolution of equation (2) gives

$$u_b(y) = -\frac{1}{2\mu}\frac{\partial p}{\partial x}(y_w^2 - y^2)\,. \tag{6}$$

3 Stability Analysis

3.1 Perturbation and dimensional analysis of the problem

Following the usual terminology of linear stability analysis, let the disturbed flow be written as a steady basic flow plus a time dependent perturbation, assumed small. We perturb the steady-state solution to look for the solution in the form

$$u^* = u_b + u \quad v^* = v \quad p^* = p_b + p\,, \tag{7}$$

where u, v, p are the small perturbations of the longitudinal and transverse speed and that of the pressure.

To evaluate the order of magnitude of different terms in the equations system, we introduce the following dimensionless variables:

$$u' = \frac{u}{u_0}, \quad v' = \frac{v}{u_0}, \quad x' = \frac{x}{H}, \quad y' = \frac{y}{H}, \quad t' = \frac{u_o}{H}t \quad \text{and} \quad p' = \frac{H}{\mu u_0}p\,. \tag{8}$$

To simplify the notation, we have used the following dimensionless variables after dropping the sign $\ll'\gg$ over the variables.

The characteristic quantities u_0 and H are fixed for a dimensionless flow rate defined by

$$\int_{-Y_w}^{Y_w} u(y)\ dy = -\frac{2}{3}\frac{\partial p}{\partial x}\,Y_w^3\,, \tag{9}$$

where $Y_w = \dfrac{y_w}{H}$.

The local Poiseuille solution which corresponds to a velocity profile across the channel section for the flow rate $Q = 4/3$ is

$$\begin{cases} \dfrac{\partial p}{\partial x} = -\dfrac{2}{Y_w^3} \\ u_b(y) = \dfrac{1}{Y_w}(1 - \dfrac{y^2}{Y_w^2})\,. \end{cases} \tag{10}$$

We introduce a perturbation stream function $\varphi(x, y, t)$, that we decompose in Fourier modes in x, to perform the standard normal mode analysis. Hereafter, we look for the solution of the perturbed equation in the form

$$\varphi(x, y, t) = F(y)e^{-i\alpha(x-ct)}\,, \tag{11}$$

where $F(y)$ is the complex amplitude of the perturbation $\varphi(x, y, t)$, α is the wave number and $c = c_r + ic_i$ is the complex wave speed.

Applying the equations (7), (8), (10) and (11) in the equations (2), (3) and (4), the dimensionless equations system of perturbations can be written as

$$\begin{aligned}[1 + i\alpha KRe(U_b - c)](\tilde{D}^2 - \alpha^2)^2F - i\alpha Re[(U_b - c)(\tilde{D}^2 - \alpha^2)\\ - (\tilde{D}^2U_b - K\tilde{D}^4U_b)]F = 0\,.\end{aligned} \tag{12}$$

The above equation needs four boundary conditions to be amenable to a numerical and/or analytical solutions such as

$$F(\pm Y_w) = \tilde{D}F(\pm Y_w) = 0\,, \tag{13}$$

where the differential operator $\tilde{D}^i$ is used instead of $\dfrac{d^i}{dy^i}$ for ease of reading.

The Reynolds number and the elasticity number are respectively defined by

$$Re = \frac{HU_0}{\nu}\,, \quad K = \frac{\beta_1}{\rho H^2}\,. \tag{14}$$

The equation (12) is valid for SO model $(K < 0)$ and for SG model $(K > 0)$.

Evidently, for the local analysis to be meaningful, the wavelength of the imposed perturbation has to be much smaller than that of the channel, i.e. $\alpha \gg n$. The (dimensionless) critical axial wavenumber for the plane Poiseuille flow is O(1) for both SO and SG fluids [14]. Hence, we limit our analysis to channels with $n = 0.1$.

3.2 Numerical solutions

In this investigation, we adopt the spectral method based on the most commonly used collocation points of Gauss-Lobatto to solve the obtained governing equation of this problem. For a complete description of this method, we refer to Canuto et *al.* [25].

We proceed to a change of variable $z = \frac{1}{Y_w}y$ to bring the interval $[-Y_w, Y_w]$ to the interval $[-1, 1]$. The equation (14) becomes

$$\begin{aligned}[1 + i\alpha KRe(U_b - c)](D^2 - \alpha^2Y_w^2)^2G(z) - i\alpha ReY_w^2[(U_b - c)\\ (D^2 - \alpha^2Y_w^2) - D^2U_b]G(z) + i\alpha ReKD^4U_bG(z) = 0\end{aligned} \tag{15}$$

with boundary conditions (14) are defined by

$$\mathbf{A}G = c\mathbf{B}G\,, \qquad G(\pm 1) = DG(\pm 1) = 0\,, \tag{16}$$

where the differential operator D^i is used instead of $\dfrac{d^i}{dz^i}$.

For specified values of K, Re, Y_w, n and α, the equation (15) with boundary conditions (16) define an eigenvalue problem for c.

In order to validate our code of calculation, we have determined the critical Reynolds number for a plane Poiseuille flow of a Newtonian fluid ($K = 0; \gamma = 0$). We find that the critical Reynolds number is $Re_c = 5772.2205$ for $\alpha_c = 1.0205$ with the number of collocation points $N = 60$. Furthermore, in Fig. 2 we plot the eigenspectrum for $Re = 2013$, $\alpha = 1.3$, $K = 0$, $\gamma = 0$ and $N = 120$. We transformed our results in spectrum to compare them with Fig. 9 of Sureshkumar [24], such that $\sigma_i = -\alpha c_r$ and $\sigma_r = \alpha c_i$. This eigenspectrum is virtually the same as that reported in Fig. 9 of Sureshkumar [24]. Hence, in this study we use $N = 120$ base functions to obtain the N-independent results.

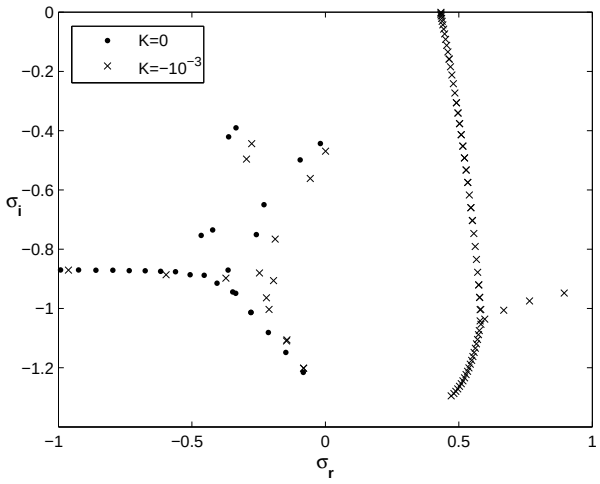

Fig. 2: Eigenspectrum for the Newtonian and SO fluid with $Re = 2013$, $\alpha = 1.3$ and $N = 120$ at $\gamma = 0$.

4 Results and Discussion

Having validated our code, we present our instability results depicting the combined effects of fluid's elasticity and the periodic channel modulation (PCM) on the stability picture and on eigenspectrum of SO ($K < 0$) and SG ($K > 0$) fluids flow.

Table 1: Variation of critical values of α, and Re versus γ at different section x for different values of K.

	$\gamma = 0.03$						$\gamma = 0.01$					
	$K = 0$		$K = -2e^{-4}$		$K = 2e^{-4}$		$K = 0$		$K = -2e^{-4}$		$K = 2e^{-4}$	
x	Re_c	α_c	Re_c	α_c	Re_c	α_c	Re_c	α_c	Re_c	$c\alpha_c$	Re_c	α_c
0	5772.22	1.020	4013.06	1.125	13390.96	0.841	5772.22	1.020	4013.06	1.125	13390.96	0.841
$\frac{\pi}{4n}$	6078.73	1.053	4216.71	1.153	14751.39	0.878	5870.64	1.031	4078.99	1.135	13806.39	0.854
$\frac{\pi}{2n}$	6215.91	1.065	4306.23	1.164	15424.44	0.892	5912.53	1.036	4106.87	1.138	13989.29	0.859
$\frac{3\pi}{4n}$	6078.73	1.053	4216.71	1.153	14751.39	0.878	5870.64	1.031	4078.99	1.135	13806.39	0.854
$\frac{\pi}{n}$	5772.22	1.020	4013.06	1.125	13390.96	0.841	5772.22	1.020	4013.06	1.125	13390.96	0.841
$\frac{5\pi}{4n}$	5500.45	0.985	3827.29	1.095	12336.53	0.799	5677.68	1.009	3949.13	1.115	13007.53	0.828
$\frac{3\pi}{2n}$	5398.34	0.970	3755.70	1.083	11978.64	0.780	5639.66	1.004	3755.27	1.111	12858.49	0.822
$\frac{7\pi}{4n}$	5500.45	0.985	3827.29	1.095	12336.53	0.799	5677.68	1.009	3949.13	1.115	13007.53	0.828
$\frac{2\pi}{n}$	5772.22	1.020	4013.06	1.125	13390.96	0.841	5772.22	1.020	4013.06	1.125	13390.96	0.841

We report in Table 1, the stability thresholds in each section of the channel corresponding to the two amplitudes of the wall $\gamma = 0.01$ and $\gamma = 0.03$ for the three fluids: Newtonian fluid ($K = 0$), SO ($K = -2e^{-4}$) and of SG ($K = 2e^{-4}$). It can be seen that for the three fluids, Re_c grows when the sections are widened and decreases when they are narrowed. This makes it possible to determine the most dangerous station $x_c = \frac{3\pi}{2n}$ which corresponds to the most narrowed section where the Re_c is minimal.

In Fig. 3 we plot the variation of Re_c depending on the section x. It is seen from this figure that, going from the relaxed section, $x = 0$, to the enlarged section $x = \frac{\pi}{2n}$, the Re_c increases, hence, the flow becomes more stable. From the section $x = \frac{\pi}{2n}$ to the the narrowed section $x = \frac{3\pi}{2n}$, the stability of the flow decreases and it regains the stable towards the section $x = \frac{2\pi}{n}$ for different values of K and γ. Therefore, we determine the most dangerous station, the most unstable flow area, $x_c = \frac{3\pi}{2n}$ which corresponds to the narrowest section where Re_c is minimal.

We present in Fig. 4 the variation of Re_c depending on the magnitude of the channel γ. Fig. 4 shows that when γ increases, the Re_c increases in the enlarged

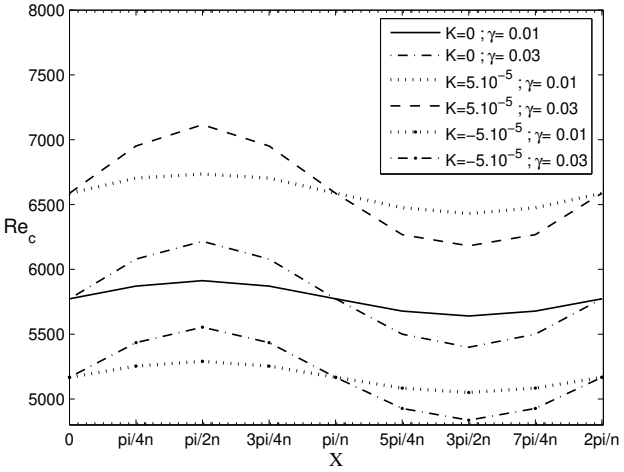

Fig. 3: Re_c versus x

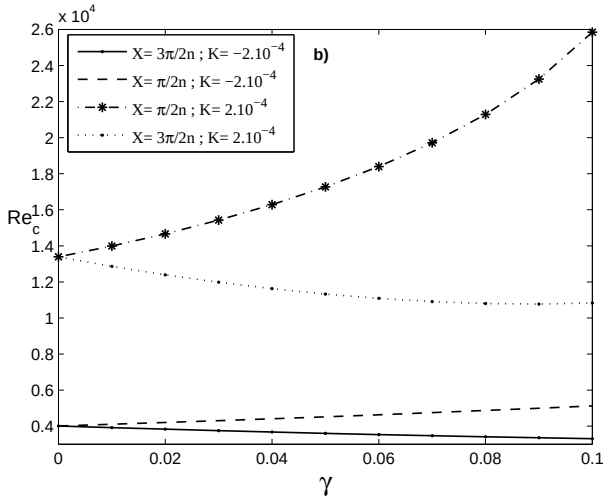

Fig. 4: Re_c versus γ.

section and decreases in the narrowed section. This result allows us to conclude that the channel amplitude has a stabilizing or destabilizing effect on the flow according to the channel section for the three types of fluids (Newtonian, SO and SG).

In the most dangerous section of the flow and for the amplitude $\gamma = 0.03$ we present in Fig. 5 the marginal stability curves of Newtonian, SO and SG fluids flow. Compared to the Newtonian fluid flow stability, the SO fluid elasticity has a destabi-

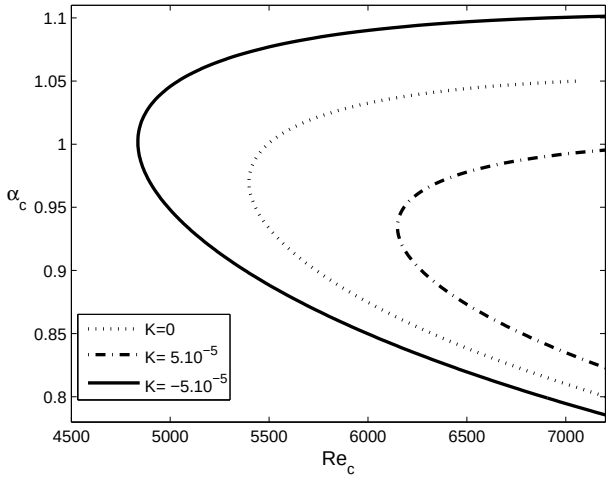

Fig. 5: Neutral stability curves for various values of the elasticity number K at $\gamma = 0.03$ and $x_c = 3p/(4n)$.

lizing effect, while that of SG fluid has a stabilizing effect.

The second part of this work is to study the effect of the fluid's elasticity K and of the amplitude of channel γ on the eigenspectrum of periodic channel flow.

Figure 6 presents the eigenspectrum of linear eigenvalue equation of SG ($K = 10^{-3}$) and that of SO ($K = -10^{-3}$) fluids for $Re = 10000$ and $\alpha = 1$ at different values of the amplitude of the channel γ. It can be seen that the Y-shaped structure of the Orr-Sommerfeld spectrum is modified by the fluid's elasticity. In addition to the continuous eigenspectum, there exist a set of continuous eigenmodes whose imaginary parts are close to $[-1/\alpha ReK]$. The magnitude of the real part of eigenvalues increases when the amplitude of the channel increases. The leading eigenvalues of the Orr-Sommerfeld spectrum of a Newtonian fluid become more stable for SG fluids and more unstable in the case of SO fluids. This result explains the destabilizing effect of the SO fluid's elasticity and stabilizing effect of that of SG fluids on the Poiseuille flow.

Figure 7 illustrates for the case of the Newtonian fluid and SG fluid that the variation of the dangerous mode in all the sections is in phase opposition with the modulation of the upper wall of the channel. This takes a minimum value in the enlarged section. This reflects that the flow of these fluids becomes more stable in this section and unstable in the narrowed section. In addition, in the case of the SO fluid, this variation is in phase with this modulation.

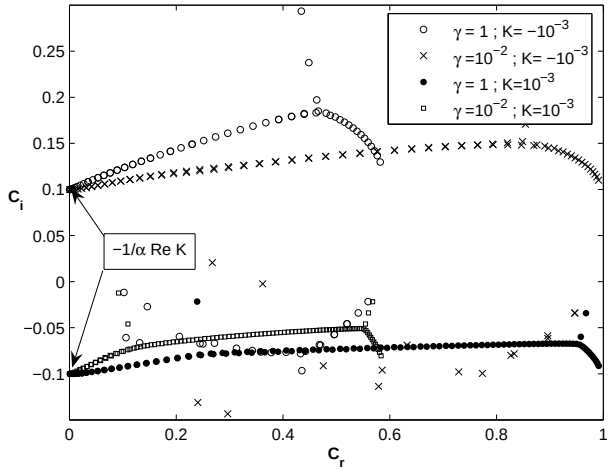

Fig. 6: Eigenspectrum for the SG and SO fluids with $Re = 10000$, $\alpha = 1$ and $N = 120$.

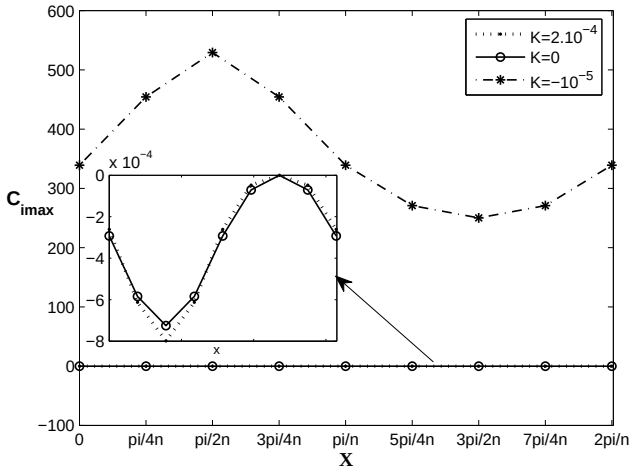

Fig. 7: Variation of the imaginary part of the most dangerous eigenmode at different section x for $\gamma = 0.01$ and Re_c corresponding of the most dangerous section.

We present separately in Fig. 8, the variations of the imaginary parts of the most unstable even and odd eigenvalues as a function of the section x. This figure shows that the imaginary parts of the even and odd eigenvalues vary in phase opposition and the imaginary part of the even eigenvalue is greater than that the odd eigenvalue.

For the SO fluid flow, Fig. 9 Show that the imaginary part of the eigenvalue is

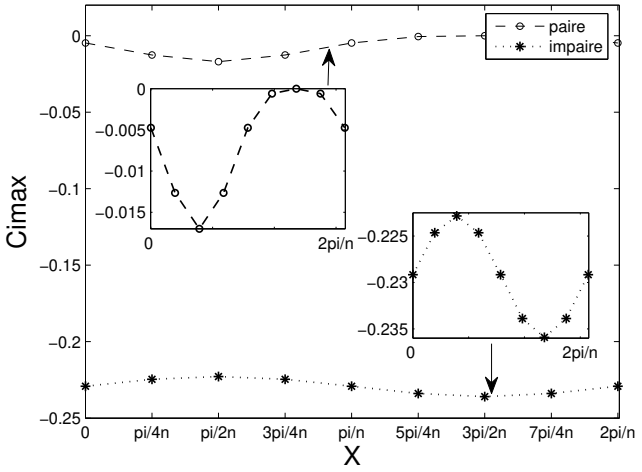

Fig. 8: Variation of the imaginary part of the most dangerous Odd and even eigenmode at different section x for SG fluid for $\gamma = 0.01$ and Re_c corresponding of the most dangerous section.

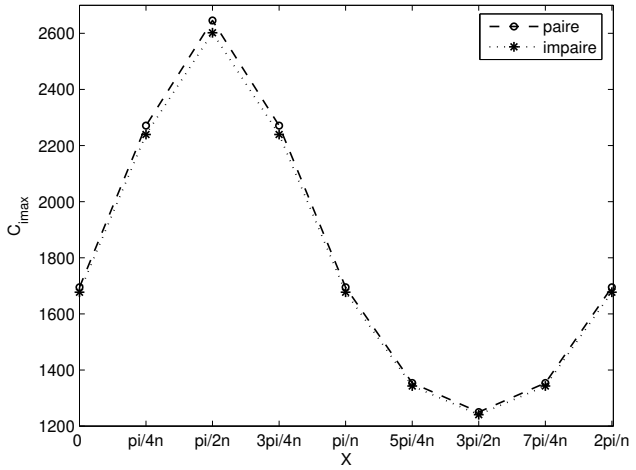

Fig. 9: Variation of the imaginary part of the most dangerous Odd and even eigenmode at different section x for SO fluid.

also greater than that of the odd eigenvalue although their variation is in the same direction. Therefore, the imaginary part of the even eigenvalue is responsible for the stability of the SG and SO fluids flow.

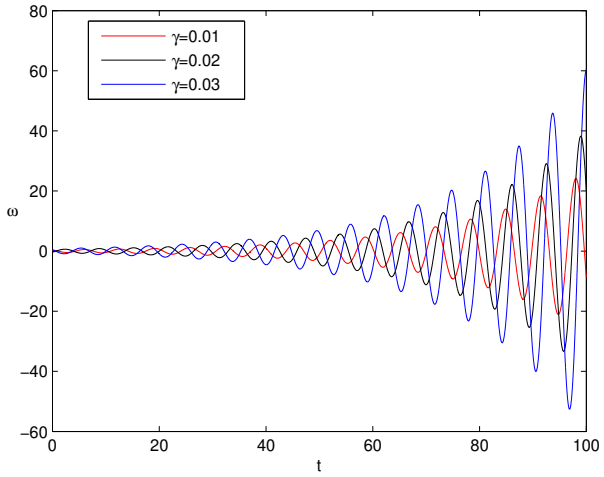

Fig. 10: Time evolution of near-wall perturbation vorticity at $x_c = 3\pi/(2n)$ as a function of γ for Poiseuille flow ($Re = 7000$, $K = -10^{-3}$, $\alpha = 1$, $\Delta t = 0.01$).

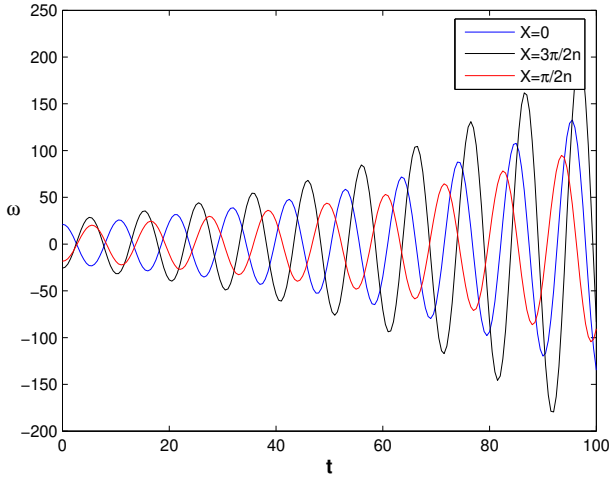

Fig. 11: Time evolution of near-wall perturbation vorticity as a function of x for Poiseuille flow ($Re = 5000$, $K = -2.10^{-3}$, $\gamma = 0.03$, $\alpha = 1$, $\Delta t = 0.5$).

In Fig. 10, we show the computed vorticity near the wall as a function of time at different values of the channel walls amplitude for the Reynolds number $Re = 7000$, the wave number $\alpha = 1$ and the elasticity number $K = -10^{-3}$. Under these conditions the flow is known to be unstable, especially, at the most unstable flow

area $x_c = \frac{3\pi}{2n}$. As seen in Fig. 10, firstly, the disturbance decays in an oscillatory fashion as expected. Secondly, in the most dangerous station x_c the increasing the channel walls amplitude destabilises the flow in the sense that the wave amplitude increases. At last, We find that this increase does not affect the frequencies of the waves, nevertheless, it develops a very small phase shift.

To highlight the existence of a critical or dangerous section x_c where the flow is more unstable, we plot in the Fig. 11 the time evolution of near-wall perturbation vorticity as a function of three sections of the channel. This figure shows that the most unstable section in this flow, corresponding to the largest amplitude of the near-wall vorticity disturbance wave, is the narrowest.

5 Conclusions

A local linear stability analysis of Poiseuille flow of both SO ($K < 0$) and SG ($K > 0$) fluids was investigated. The critical numerical values of the Reynolds number Re_c, the critical wave number α_c and the wave speed $c = c_r + ic_i$ were obtained for several selected values of the channel amplitude, γ, and the elasticity number K.

We conclude that: in the one hand, the SO fluid's elasticity has a destabilizing effect on the local Poiseuille flow, while that of SG fluid has a stabilizing effect. Moreover, the critical axial location is $x_c = 3\pi/(2n)$ for the three fluids, Newtonian ($K = 0$), SO ($K < 0$) and SG ($K > 0$). Compared to the local stability of the fluids flow in the relaxed channel region ($\gamma = 0$), we showed that, the channel amplitude γ has a stabilizing effect on the flow in the extended channel region and has a destabilizing effect on the narrowed channel region. In the other hand, the examination of eigenspectrum of the SO and SG fluids models reveals that Y-shaped structure of Orr-Sommerfeld spectrum is modified by fluid's elasticity. In addition, the study of the eigenspectrum proved the existence of two families of eigenmodes, whose imaginary parts are close to $[-1/\alpha ReK]$: The first is stable corresponding to the SG fluid flow and the second is unstable corresponding to the SO fluid flow. Moreover, we have studied the evolution of the imaginary part of the most dangerous eigenvalue. This allowed us to observe that this evolution in the case of the SG fluid is in accordance with the geometrical modulation of the channel, whereas that of the SO fluid is non-compliant with this modulation. This study also confirms that the dangerous mode is the evenmode. At last, the investiguation of the time evolution of the near-wall vorticity of the perturbed SO fluid flow, highlights the destabilizing effect of the channel amplitude γ and the existence of a more dangerous station $x_c = 3\pi/(2n)$ which corresponds to the most narrowed section where the amplitude of the near-wall vorticity disturbance wave is largest.

REFERENCES

[1] B.A. TOMS (1948) Observations on the flow of linear polymer solutions through straight tubes at large Reynolds numbers. *Proceedings of International Rheologigal Congress Holand* **12** 135-141

[2] D.H. CHUN, W.H. SCHWARZ (1968) Stability of plane Poiseuille flow of a second-order fluid. *Physics of Fluids* **11** 5-9

[3] K. SADEGHY, S.M. TAGHAVI, N. KHABAZI, M. MIRZADEH, I. KARIMFAZLI (2007) On the use of hydrodynamic instability test as an efficient tool for evaluating viscoelastic fluid models. *ASME Journal of Basic Engineering* **1** 367-379

[4] A. RAFIKI, A. HIFDI (2012) Stability of plane Poiseuille flow of viscoelastic fluids in the presence of a transverse magnetic field. *MATEC Web of Conferences* **1** 06006

[5] A. RAFIKI, A. HIFDI, M.T. OUAZZANI, S.M. TAGHAVI (2014) Hydrodynamic stability of Poiseuille flow of non-Newtonian fluids in the presence of a transverse magnetic field. *Journal of the Society of Rheology Japan* **42** No. 1 51-60

[6] C. FETECAU (2005) Starting solution for some unsteady unidirectional flows of a second grade fluid. *International Journal of Engineering Science* **43** 781-789

[7] N.S. KHAN, T. GUL, S. ISLAM, W. KHAN (2017) Thermophoresis and thermal radiation with heat and mass transfer in a magnetohydrodynamic thin-film second-grade fluid of variable proprieties past a stretching sheet. *The european Physical Journal Plus* **132** No. 11

[8] M.I. ASJAD, N.A. SHAH, M. ALEEM, I. KHAN (2017) Heat transfer analysis of fractional second-grade fluid subject to Newtonian heating with caputo and Caputo-Fabrizio fractional derivatives: A comparison. *The european Physical Journal Plus* **132** No. 340

[9] R. FOSDICK, K. RAJAGOPAL (1979) Anomalous features in the model of second-order fluids. *Archive for Rational Mechanics and Analysis* **70** 145-152

[10] J. DUNN, K. RAJAGOPAL (1995) Fluids of differential type : critical review and thermodynamic analysis. *International Journal of Engineering Science* **33** 689-729

[11] C. FOIAS, D.D. HOLM, E.S. TITI (2001) The Navier-Stokes-alpha model of fluid turbulence. *Physica D* **152-153** 505-519

[12] E. LUNASIN, S. KURIEN, M.A. TAYLOR, E.S. TITI (2007) A study of the Navier-Stokes-alpha model for two-dimensional turbulence. *Journal of Turbulence* **8** No. 30 1-21

[13] D.D. HOLM (1999) Fluctuation effects on 3D Lagrangian mean and Eulerian mean fluid motion. *Physica D* **133** 215-269

[14] S. Y. CHEN, C. FOIAS, D.D. HOLM, E.J. OLSON, E.S. TITI, S. WYNNE (1998) The Camassa-Holm equations as a closure model for turbulent channel and pipe fows. *Physical Review Letters* **81** 5338-5341

[15] S.Y. CHEN, C. FOIAS, D.D. HOLM, E.J. OLSON, E.S. TITI, S. WYNNE (1999) The Camassa-Holm equations and turbulence in pipes and channels. *Physica D* **133** 49-65

[16] S.Y. CHEN, C. FOIAS, D.D. HOLM, E.J. OLSON, E.S. TITI, S. WYNNE (1999) A connection between the Camass-Holm equations and turbulence in pipes and channels. *Physics of Fluids* **11** 2343-2353

[17] R. CAMASSA, D.D. HOLM (1993) An integrable shallow water equation with peaked solitons. *Physical Review Letters* **71** 1661-1664

[18] R.S. RIVLIN, J.L. ERICKSON (1955) Stress-deformation relations for isotropic materials. *Journal of Rational Mechanics and Analysis* **4** 323-425

[19] D.F. JAMES, D.R. MCLAREN (1975) The laminar flow of dilute polymer solutions through porous media. *Journal of Fluid Mechanics* **70** 733-752

[20] D.F. JAMES, N. PHAN-THEIN, M.N.K. KHAN, A.N. BERIS, S. PILITSIS (1990) Flow of test fluid M1 in corrugated tube. *Journal of non Newtonian Fluid Mechanics* **35** 405-412

[21] R. ZHENG, N. PHAN-THEIN, R.I. TANNER, M.B. BUSH (1990) Numerical analysis of viscoelastic flow through a sinusoidally corrugated tube using a boundary element method. *Journal of Rheology* **34** 79-102

[22] R.C. YALAMANCHIL, A. SRIVAT, K.R. RAJAGOPAL (1995) An experimental investigation of flow of dilute polymer solutions through corrugated channels. *Journal of non Newtonian Fluid Mechanics* **58** 243-277

[23] T. KOSHIBA, N. MORI, K. NAKAMURA (19596) Viscoelastic effects of the flow of polymer solutions in periodic undulating channels. *Proceedings of the XIIth International Congress on Rheology* 381-382

[24] R. SURESHKUMAR (2001) Local linear stability characteristics of viscoelastic periodic channel. *Journal of non Newtonian Fluid Mechanics* **97** 125-148

[25] C. CANUTO, M.Y. HUSSAINI, A. QUARTERONI, T.A. ZANG (1988) "Spectral Methods in Fluid Dynamics". New York: Springer-Verlag

[26] S.A. ORSZAG (1980) Spectral methods for problems in complex geometries. *Journal of Computational Physics* **37** 70

[27] K.Z. KORCZAK, A.T. PATERA (1986) An isoparametric spectral element method for solution of the Navier-Stokes equations in complex geometry. *Journal of Computational Physics* **62** 361